Electron-transfer reactions in the Marcus inverted region. Charge recombination versus charge shift reactions

ARTICLE *in* JOURNAL OF THE AMERICAN CHEMICAL SOCIETY · MARCH 1989

Impact Factor: 12.11 · DOI: 10.1021/ja00187a077

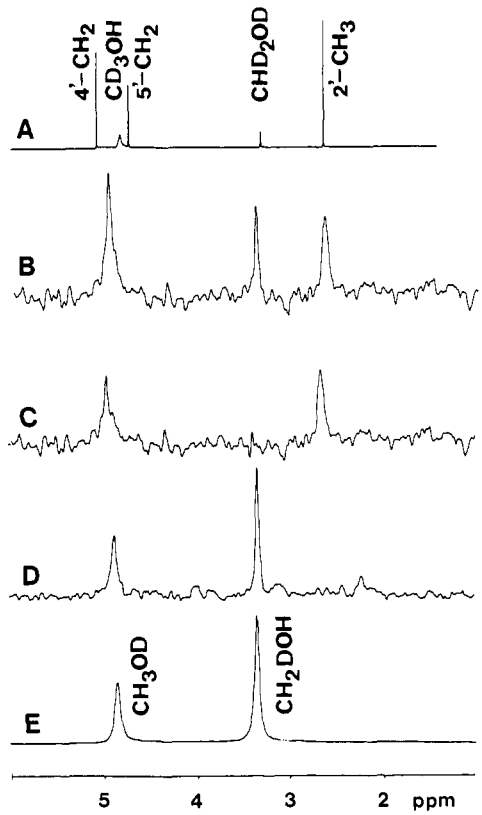

Figure 1. (A) Low-frequency region of the 500.13 MHz ^1H NMR spectrum of pyridoxol hydrochloride (in deuteriomethanol). (B) 76.775 MHz ^2H NMR spectrum of pyridoxol hydrochloride (ca. 1.7 mg in 50 μL of methanol) obtained from *E. coli* B WG2 after incubation with D-1-deoxy[1,1,1-$^2H_3$,(*RS*)-5-$^2H_1$]xylulose. (C) Difference spectrum (B minus E). (D) 76.775 MHz ^2H NMR spectrum of pyridoxol hydrochloride (ca. 1.7 mg in 50 μL of methanol) obtained from *E. coli* B WG2 after incubation with L-1-deoxy[1,1,1-$^2H_3$,(*RS*)-5-$^2H_1$]xylulose (experiment 2). (E) 76.775 MHz ^2H NMR spectrum (natural abundance) of methanol. The spectra were determined on a Bruker AM 500 spectrometer. Spectral parameters: spectral width, 2000 Hz; memory size, 16 K; pulse flip angle, 45°. To obtain adequate signal-to-noise ratio in the deuterium spectra (B and D) more than 25 000 transients were required.

Scheme I

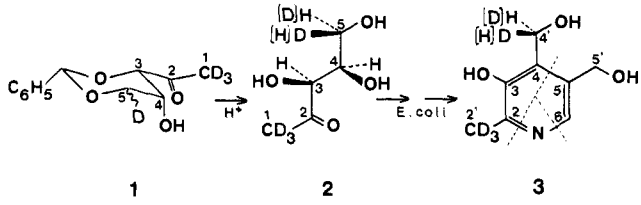

(c.f., ^1H NMR spectrum of pyridoxol hydrochloride, Figure 1A). The second signal, at δ 3.30 ppm, corresponds to the natural abundance deuterium signal of the -CDH_2 group of the solvent (c.f., natural abundance ^2H NMR spectrum of methanol, Figure 1E). The third signal, at δ 4.95 ppm, located at a chemical shift corresponding both to the C-4′ hydroxymethyl protons of pyridoxol HCl (c.f., Figure 1A) as well as to that of the -OD group of the solvent (c.f., Figure 1E), is in fact a composite of both, as shown by the difference spectrum (Figure 1C, i.e., B minus E).

Thus, deuterium from the deuteriated sample of D-1-deoxyxylulose entered the predicted sites, C-2′ and C-4′, and only the predicted sites, of pyridoxol hydrochloride. Furthermore, since L-1-deoxyxylulose did not deliver deuterium into the vitamin, the incorporation of deuterium is stereochemically controlled.

These results lead to the inference that the intact C_5 skeleton of D-1-deoxyxylulose (**2**) enters pyridoxol (**3**) to supply the C_5 unit, C-2′,-2,-3,-4,-4′. If carbon–carbon cleavage of the precursor molecule, into a C_2 and a C_3 unit, had occurred prior to entry into pyridoxol, then deuterium would have been incorporated not only into C-2′ and C-4′, as observed, but also into C-5′ (c.f., ref 3).

Because of the superposition of signals at δ 4.95 ppm in the ^2H NMR spectrum of labeled pyridoxol hydrochloride in methanol (Figure 1B) and the unfavorable signal-to-noise ratio in the difference spectrum (Figure 1C) the ratio, signal area at δ 2.54 ppm (CD_3)/signal area at δ 4.95 ppm (CDH-4′), cannot be determined with precision. Intact incorporation of precursor into pyridoxol demands that this ratio be 3 (see ref 8). The observed value (Figure 1C) can be estimated to be <3 but >2.

Even though it is now demonstrated that the intact carbon skeleton of D-1-deoxyxylulose enters the C_5 unit, C-2′,-2,-3,-4,-4′, of pyridoxol, the question still remains whether the compound itself, or the corresponding 4-oxo derivative, lies on the direct route into pyridoxol from the C_2 and C_3 units, pyruvate and dihydroxyacetone phosphate, that give rise to the C-2′,-2 and C-3,-4,-4′ moieties, respectively.[6,7]

It is of interest that D-1-deoxyxylulose, which is now shown to be implicated in the biosynthesis of vitamin B_6 in *E. coli*, also serves as a precursor of the thiazole unit of vitamin B_1 in the same organism[9] and that a D-1-deoxypentulose has been postulated as an intermediate of the biosynthesis of vitamin B_2.[10]

Acknowledgment. This work was supported by grants from the Medical Research Council of Canada (to R.E.H.) and the Natural Sciences and Engineering Research Council of Canada (to I.D.S.). We thank Dr. Tomasz Kozluk for the preparation of the deuterium-labeled samples of D- and L-1-deoxyxylulose and Richard Pauloski for skilled technical assistance.

(9) David, S.; Estramareix, B.; Fischer, J.-C.; Therisod, M. *J. Chem. Soc., Perkin Trans. 1*, **1982**, 2131-2137.
(10) Volk, R.; Bacher, A. *J. Am. Chem. Soc.* **1988**, *110*, 3651-3653.

Electron-Transfer Reactions in the Marcus Inverted Region. Charge Recombination versus Charge Shift Reactions

Ian R. Gould,* Jacques E. Moser, Bruce Armitage, and Samir Farid*

Corporate Research Laboratories
Eastman Kodak Company
Rochester, New York 14650-2109

Joshua L. Goodman* and Michael S. Herman

Chemistry Department, University of Rochester
Rochester, New York 14627
Received November 14, 1988

The recent experimental verification[1] of the Marcus inverted region[2] has stimulated renewed theoretical interest in electron-transfer processes. Kakitani and Mataga[3] have described a model in which partial solvent dielectric saturation of ionic species involved in electron-transfer reactions results in a negligible decrease in rate in the inverted region for reactions in which two neutral species yield two ionic species (termed charge separation reactions, CS). The model also predicts a pronounced inverted region for charge recombination reactions (CR) in which two ions yield two neutral species and intermediate behavior for charge shift (CSH)

(1) (a) Closs, G. L.; Miller, J. R. *Science* **1988**, *240*, 440. (b) Miller, J. R.; Beitz, J. V.; Huddleston, R. K. *J. Am. Chem. Soc.* **1984**, *106*, 5057. (c) Wasielewski, M. R.; Niemczyk, M. P.; Svec, W. A.; Pewitt, E. B. *J. Am. Chem. Soc.* **1985**, *107*, 1080. (d) Irvine, M. P.; Harrison, R. J.; Beddard, G. S.; Leighton, P.; Sanders, J. K. M. *Chem. Phys.* **1986**, *104*, 315. (e) Ohno, T.; Yoshimura, A.; Mataga, N. *J. Phys. Chem.* **1986**, *90*, 3295.
(2) (a) Marcus, R. A. *J. Chem. Phys.* **1956**, *24*, 966. (b) Marcus, R. A. *Discussions Faraday Soc.* **1960**, *29*, 21.
(3) (a) Kakitani, T.; Mataga, N. *J. Phys. Chem.* **1987**, *91*, 6277. (b) Kakitani, T.; Mataga, N. *J. Phys. Chem.* **1986**, *90*, 993. (c) Kakitani, T.; Mataga, N. *Chem. Phys.* **1985**, *93*, 381.

0002-7863/89/1511-1917$01.50/0

Table I. Quantum Yields for Free Radical Ion Formation from *N*-Methylacridinium Radical/Alkylbenzene Radical Cation Pairs in Acetonitrile at 25 °C

alkylbenzene	ΔG_{-et}	Φ_{sep}(ta)[a]	Φ_{sep}(pa)[b]	k_{-et}/k_{sep}[c]
m-xylene	−2.59	0.27	0.26	2.7
o-xylene	−2.59	0.27	0.28	2.7
mesitylene	−2.56	0.19	0.15	4.3
p-xylene	−2.51	0.16	0.14	5.4
1,2,4-trimethylbenzene	−2.37	0.084	0.08	10.9
1,2,3,4-tetramethylbenzene	−2.29	0.054		17.7
1,2,3,5-tetramethylbenzene	−2.29	0.049		19.6
1,4-dimethyltetrahydronaphthalene	−2.26	0.051		18.8
durene	−2.23	0.042	0.05	22.8
octahydrophenanthrene	−2.22	0.044		21.7
octahydroanthracene	−2.17	0.039		24.7
pentamethylbenzene	−2.16	0.037		26.0
hexamethylbenzene	−2.04	0.031		31.3

[a] Quantum yield measured using transient absorption spectroscopy. [b] Quantum yield measured using pulsed photoacoustic calorimetry.[7] [c] Calculated from Φ_{sep}(ta) using eq 2.

reactions in which no net charge change takes place. However, no direct comparison, using similar chemical systems, of these different types of reactions in the inverted region has yet been reported.

We have shown that return electron transfer within photochemically generated geminate radical ion pairs provides a good example of the inverted region and that subtle molecular effects can be observed.[4] We now compare directly CSH and CR reactions in such systems (eq 1a and 1b), in which the differences

$$A + D \underset{k_{-et}\,(CR)}{\overset{h\nu}{\rightleftharpoons}} A^{\bullet-}/D^{\bullet+} \xrightarrow{k_{sep}} A^{\bullet-} + D^{\bullet+} \qquad (1a)$$

$$A^{+} + D \underset{k_{-et}\,(CSH)}{\overset{h\nu}{\rightleftharpoons}} A^{\bullet}/D^{\bullet+} \xrightarrow{k_{sep}} A^{\bullet} + D^{\bullet+} \qquad (1b)$$

in molecular structure, reaction free energy, and reaction conditions are minimal. Previously, a transient absorption technique was used to determine the quantum yields for separated ion formation, Φ_{sep}, from which the rates of return electron transfer (k_{-et}, eq 1) were obtained.[4] We now also report the use of pulsed photoacoustic calorimetry in which the thermodynamics of the electron-transfer reactions are monitored.[5]

Quenching of the first singlet excited states of the uncharged acceptors 9,10-dicyanoanthracene (DCA) and 2,6,9,10-tetracyanoanthracene (TCA) with the alkylbenzene donors listed in Table I results in the formation of geminate radical ion pairs ($A^{\bullet-}/D^{\bullet+}$).[4] The values of Φ_{sep}, determined previously for these pairs,[4] depend upon the rates of return electron transfer, which in this case are CR reactions (k_{-et}, eq 1a). The molecular dimensions, reduction potential, and excited state properties of *N*-methylacridinium (MA^+) are similar to those of TCA.[6] In this case, since the acceptor is positively charged, quenching of its first excited singlet state by the alkylbenzene donors leads to radical/radical cation pairs ($A^{\bullet}/D^{\bullet+}$); thus the return electron-transfer reaction is a CSH type (eq 1b). Values of Φ_{sep} for this system were determined by using both the transient absorption[4]

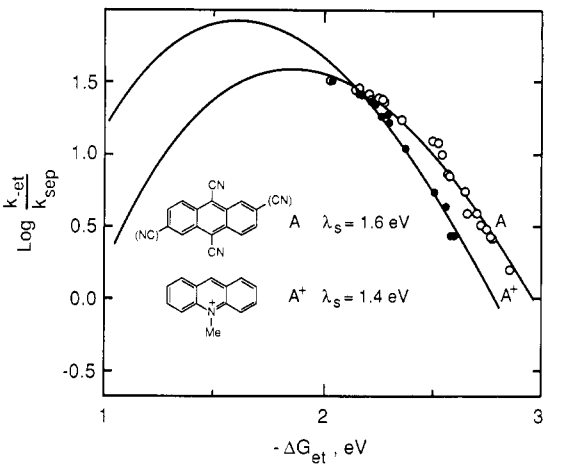

Figure 1. The ratio of the rates of return electron transfer and separation (k_{-et}/k_{sep}) for (A) the charge recombination (CR) reaction between cyanoanthracene radical anions and alkylbenzene radical cations and (B) the charge shift (CSH) reaction between *N*-methylacridinium radicals and alkylbenzene radical cations, as a function of the electron-transfer reaction free energy (ΔG_{-et}) in acetonitrile at 25 °C.

and photoacoustic[7] methods. The results (Table I) demonstrate that the two techniques give very similar results, despite the fact that each uses different actinometers.[8]

The quantum yields are related to k_{sep} and k_{-et} as shown in eq 2. Although the separation rate is expected to be higher in the

$$\frac{k_{-et}}{k_{sep}} = \frac{1}{\Phi_{sep}} - 1 \qquad (2)$$

case of the acridinium acceptor, since there is no coulombic attraction to overcome in the radical/cation pair as in the anion/cation pair, this rate is likely to be constant within each set of data. Changes in the quantum yields, therefore, are due to changes in the rates of return electron transfer, which decrease as the exothermicity of the reaction increases, i.e., ΔG_{-et} decreases. ΔG_{-et} is given by the negative of the energy stored in the ion pair, E_{ox}(donor) − E_{red}(acceptor).[4] In Figure 1 are plotted the rate ratios k_{-et}/k_{sep} for both the CR and CSH reactions, as a function of ΔG_{-et}.

The data can be analyzed as before[4] using a semiclassical theory of electron-transfer reactions[9] in which the reaction rate is described as the product of a relative Franck–Condon factor (FC)[1b]

$$\frac{k_{-et}}{k_{sep}} = P \cdot FC \qquad (3a)$$

$$FC = \sum_{w=0}^{\infty} (e^{-S}S^{w}/w!)\, \exp\{-[(\lambda_s + \Delta G_{-et} + wh\nu)^2/4\lambda_s k_b T]\} \qquad (3b)$$

$$S = \lambda_v/h\nu$$

$$P = (\pi/\hbar^2\lambda_s k_b T)^{1/2}|V|^2/k_{sep} \qquad (3c)$$

(4) (a) Gould, I. R.; Ege, D.; Mattes, S. L.; Farid, S. *J. Am. Chem. Soc.* **1987**, *109*, 3794. (b) Gould, I. R.; Moser, J. E.; Ege, D.; Farid, S. *J. Am. Chem. Soc.* **1988**, *110*, 1991. (c) Gould, I. R.; Moody, R.; Farid, S. *J. Am. Chem. Soc.* **1988**, *110*, 7242. (d) Gould, I. R.; Farid, S. *J. Am. Chem. Soc.* **1988**, *110*, 7883. (e) Separated radical cations are scavenged by added dimethoxystilbene (DMS, 5×10^{-4} M); Φ_{sep}(ta) are obtained from the size of the transient absorbance due to the DMS radical cation, monitored at 530 nm (ref 4a–d).

(5) (a) Goodman, J. L.; Peters, K. S. *J. Am. Chem. Soc.* **1986**, *108*, 1700. (b) Ci, X.; daSilva, R. S.; Goodman, J. L.; Nicodem, D. E.; Whitten, D. G. *J. Am. Chem. Soc.*, in press. (c) LaVilla, J. A.; Goodman, J. L. *Chem. Phys. Lett.* **1987**, *141*, 149.

(6) The excited state energies and lifetimes for DCA, TCA, and MA^+ are 2.88, 2.82, and 2.77 eV and 15, 17, and 36 ns, respectively. The ground-state reduction potentials are −0.89, −0.45, and −0.46 V vs SCE in methylene chloride at 25 °C. Using perchlorate, tetrafluoroborate, or hexafluorophosphate counter ions for MA^+ had no effect on the results; the hexafluorophosphate salt was used for most of the studies. It is assumed that the MA^+ cation and gegen ion are dissociated under the conditions of dilute solution in a polar solvent.

(7) The photoacoustic apparatus has been described previously.[5c] The Φ_{sep}(pa) were determined by using the equation, Φ_{sep}(pa) = $(1 - \Phi_f - \alpha)E_{h\nu}/E_{rip}$, in which Φ_f is the fluorescence quantum yield, α is the fraction of the photon energy released as heat in the reaction, $E_{h\nu}$ is the photon energy, and E_{rip} is the energy of the radical ions, given by E_{ox}(donor) − E_{red}(acceptor).[4] Experimental waveforms were obtained from photolysis (410 nm, 69.8 kcal/mol) of argon-degassed, acetonitrile solutions containing MA^+ (OD ~ 0.3–0.7) and the substituted benzenes (0.2 M). Analysis using calibration waveforms obtained from photolysis of similar solutions containing ferrocene gave the experimental α values.[5c] Experiments were also performed with added 4,4′-dimethoxystilbene (DMS, 1×10^{-3} M) which results in secondary electron transfer from DMS to the radical cation of the substituted benzenes.[4] By using this method, knowledge of the absolute energies of each of the geminate pairs is not necessary. Both methods gave similar Φ_{sep}(pa). Averages of the values obtained by using the two methods are given in Table I.

(8) The two techniques also gave similar quantum yields for Φ_{sep} from the $A^{\bullet-}/D^{\bullet+}$ pairs (eq 1a).

(9) (a) Van Duyne, R. P.; Fischer, S. F. *Chem. Phys.* **1974**, *5*, 183. (b) Ulstrup, J.; Jortner, J. *J. Chem. Phys.* **1975**, *63*, 4358. (c) Siders, P.; Marcus, R. A. *J. Am. Chem. Soc.* **1981**, *103*, 741, 748.

and a term including an electronic coupling matrix element squared (V^2). The rate ratio k_{-et}/k_{sep} is thus described as the product of FC and a term P which is a dimensionless adjustable scaling parameter that includes the separation rate (eq 3c). The dependence of the rate ratio on ΔG_{-et} and the solvent and vibrational reorganization energies, λ_s and λ_v, are contained in FC. The reorganization energies are adjustable, as is a final parameter, ν, which is a single averaged frequency taken as representative of the rearranged vibrational modes. In fitting the data it is assumed that values for λ_v and ν of 0.3 eV and 1500 cm^{-1}, respectively, are appropriate for both sets of data.[4] The fitting procedure thus involves finding the best values for P and λ_s. The value of λ_s which gives the best fit to the CSH data, 1.4 eV, is smaller than that for the CR data, 1.6 eV.[10]

It is clear from Figure 1 that both sets of data can be described very well by the same semiclassical formalism in which the effects of solvent dielectric saturation are not included.[11] Indeed, in the free energy range in which the data are obtained (ca. −2.0 to −2.6 eV, Figure 1) the decrease in rate with increasing exothermicity of the CSH reaction is even *more pronounced* than that of the CR reaction, although the fitting procedure reveals that this is due to the somewhat smaller λ_s for the CSH reaction. Thus, the present study demonstrates that when CR and CSH reactions in geminate pairs are compared directly using similar chemical systems, the prediction[3] that the inverted region for the CSH reactions should be less pronounced than that for the CR reactions is not sustained. This finding for solvent-separated pairs is in agreement with similar conclusions obtained by Marcus[12] for electron-transfer reactions in contact ion pairs based upon comparisons between absorption and emission spectra of CT complexes.

Acknowledgment. The work at the University of Rochester was supported by the National Science Foundation (CHE-871370). The authors thank R. A. Marcus for providing a preprint of his work and for valuable discussions.

(10) Although the difference in λ_s of 0.2 eV may not be very accurate due to limitations in the electron-transfer model and the assumptions involved in the fitting procedure, the total reorganization energy for the CSH reaction is clearly somewhat smaller than that for the CR reaction.

(11) A referee points out that a more pronounced inverted region would be predicted for the CSH reaction if both MA^+ and the MA radical were similarly solvated. We feel that this is unlikely in the polar acetonitrile solvent.

(12) Marcus, R. A. *J. Phys. Chem.*, in press.

Variational Transition State for the Reaction of Cl_2C: with Ethylene and the Thermodynamics of Carbene Additions

James F. Blake, Scott G. Wierschke, and William L. Jorgensen*

Department of Chemistry, Purdue University West Lafayette, Indiana 47907

Received September 2, 1988

According to conventional transition state theory, the transition state for a reaction is located at the potential energy maximum along the minimum energy reaction path (MERP). However, this definition can lead to serious errors in computed rate constants.[1] The most relevant point is actually the maximum in the free energy of activation curve or "variational transition state" (VTS).[1] Many of the dynamical consequences of free energy of activation maxima have been studied for atom-transfer reactions using mostly semiempirical potential energy surfaces[1] and a few ab initio surfaces.[2] Houk and co-workers[3] have now proposed that differences in the locations of the conventional and variational transition states can rationalize two intriguing aspects of carbene additions to alkenes: observations of negative activation energies[4] and entropy control of selectivity.[5] Their proposals stemmed from results of ab initio 3-21G calculations, particularly for $^1CCl_2$ plus ethylene, which indicated that π-complexes are not intermediates in reactions of relatively reactive halocarbenes with alkenes.[3] The use of the 3-21G basis set in this context raises concern since it does not include d-orbitals which are accepted as critical to the electronic structure of small rings.[6] Accordingly, in order to better test the basis of their model and to provide a more reliable gas-phase energy surface, ab initio calculations have been carried out for $^1CCl_2 + H_2C{=}CH_2$ including d-orbitals and electron correlation in the geometry optimizations. Subsequent calculations of vibrational frequencies yielded the free energy of activation curve and VTS.

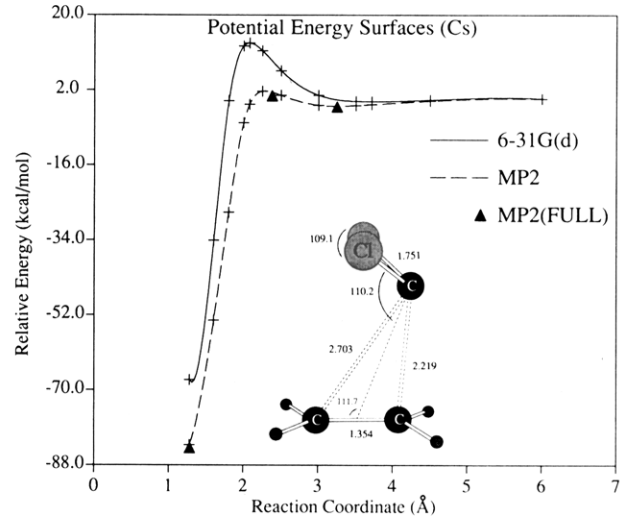

Figure 1. Computed potential energy surfaces. Inset: key geometrical parameters for the MP2(FULL)/6-31G(d) optimized transition state.

The reaction coordinate, r_c, is defined as the distance between the carbene carbon and the center of the CC bond in ethylene.[3] A MERP was obtained by geometry optimizations in C_s symmetry with the 6-31G(d) basis set at fixed values of r_c.[6,7] Four stationary points (reactants, π-complex, transition state, and product) were located and confirmed by frequency calculations. The effect of electron correlation was then estimated by single-point calculations with MP2 theory in the frozen core approximation for each 6-31G(d) optimized geometry.[6] In view of the pronounced correlation effects, the stationary points were reoptimized including the correlation energy at the MP2(FULL)/6-31G(d) level[6] on a Cray XMP. Frequency calculations were carried out for nine of the 6-31G(d) optimized points to compute the zero-point corrections, enthalpies, and entropies needed to construct the free energy of activation profile.[6,8]

(1) (a) Truhlar, D. G.; Garrett, B. C. *Acc. Chem. Res.* **1980**, *13*, 440. (b) Truhlar, D. G.; Hase, W. L.; Hynes, J. T. *J. Phys. Chem.* **1983**, *87*, 2664. (c) Kreevoy, M. M.; Truhlar, D. G. In *Investigations of Rates and Mechanisms of Reactions*; Bernasconi, C., Ed.; Wiley: New York, 1986; Vol. 6, Part 1, p 13. (d) Truhlar, D. G.; Garrett, B. C. *J. Chim. Phys.* **1987**, *84*, 365.

(2) (a) Truhlar, D. G.; Isaacson, A. D.; Skodje, R. T.; Garrett, B. C. *J. Phys. Chem.* **1982**, *86*, 2252. (b) Isaacson, A. D.; Truhlar, D. G. *J. Chem. Phys.* **1982**, *76*, 1380. (c) Garrett, B. C.; Truhlar, D. G.; Wagner, A. F.; Dunning, T. H., Jr. *J. Chem. Phys.* **1983**, *78*, 4400. (d) Truhlar, D. G.; Grev, R. S.; Garrett, B. C. *J. Phys. Chem.* **1983**, *87*, 3415. (e) Doubleday, C.; McIver, J.; Page, M.; Zielinski, T. *J. Am. Chem. Soc.* **1985**, *107*, 5800.

(3) (a) Houk, K. N.; Rondan, N. G.; Mareda, J. *J. Am. Chem. Soc.* **1984**, *106*, 4291. (b) Houk, K. N.; Rondan, N. G. *J. Am. Chem. Soc.* **1984**, *106*, 4293. (c) Houk, K. N.; Rondan, N. G.; Mareda, J. *Tetrahedron* **1985**, *41*, 1555.

(4) (a) Zupancic, J. J.; Schuster, G. B. *J. Am. Chem. Soc.* **1981**, *103*, 944. (b) Turro, N. J.; Lehr, G. F.; Butcher, J. A., Jr.; Moss, R. A.; Guo, W. *J. Am. Chem. Soc.* **1982**, *104*, 1754.

(5) (a) Skell, P. S.; Cholod, M. S. *J. Am. Chem. Soc.* **1969**, *91*, 7131. (b) Giese, B.; Lee, W.-B.; Neumann, C. *Angew. Chem., Int. Ed. Engl.* **1982**, *21*, 310.

(6) Hehre, W. J.; Radom, L.; Schleyer, P. v. R.; Pople, J. A. *Ab Initio Molecular Orbital Theory*; Wiley: New York, 1986.

(7) Binkley, J. S.; Whiteside, R. A.; Raghavachari, K.; Seeger, R.; Defrees, D. J.; Schlegel, H. B.; Frisch, M. J.; Pople, J. A.; Kahn, L. R. GAUSSIAN 82, Release H; Carnegie-Mellon University: Pittsburgh, PA, 1982.

0002-7863/89/1511-1919$01.50/0